Desalination and Water Treatment
www.deswater.com
doi: 10.1080/19443994.2014.925836

55 (2015) 1167–1176
July

Taylor & Francis
Taylor & Francis Group

PVDF/PMMA membranes for lemon juice clarification: fouling analysis

Leticia R. Firmán[a], Cecilia Pagliero[a], Nelio A. Ochoa[b], José Marchese[b,*]

[a]*Departamento de Tecnología Química, Universidad Nacional de Río Cuarto, CONICET, Ruta 36, Km 601, 5800 Río Cuarto, Córdoba, Argentina, emails: lfirman@ing.unrc.edu.ar (L.R. Firmán), cpagliero@ing.unrc.edu.ar (C. Pagliero)*
[b]*Universidad Nacional de San Luis, INFAP (CONICET) Chacabuco y Pedernera, San Luis 5700, Argentina, Tel. +54 266 4446211; emails: aochoa@unsl.edu.ar (N.A. Ochoa), marchese@unsl.edu.ar (J. Marchese)*

Received 21 November 2013; Accepted 12 May 2014

ABSTRACT

Microfiltration/ultrafiltration membranes with different degrees of hydrophilicity and structural characteristics from poly(vinylidene fluoride) (PVDF), polymethylmetacrylate (PMMA), and polyvinylpirrolidone (PVP) in dimethylformamide (DMF) solvent were prepared to be used in the lemon juice clarification. The effect of transmembrane pressure ($\Delta p = 0.4$–1 bar) and tangential feed velocity ($v = 0.2$–1 m/s) on permeate flux and juice quality at $T = 20$°C was examined. The membrane containing 15% of PVDF, 5% PMMA, and 5% PVP (mean pore radii $r_{pm} = 0.25$ μm and porosity $\varepsilon = 0.25$) achieved the best performance at $\Delta p = 1$ bar and $v = 1$ m/s, with a final permeate flux at quasi-steady state of 32.5 (L/hm^2). The clarified lemon juice presented physical, chemical, and nutritional characteristics comparable to the fresh lemon juice, and 100% of total solid rejection. Membrane fouling was evaluated by applying different fouling models. Results indicated that a good fitting correlation between the experimental data and both complete blocking and cake models was achieved.

Keywords: Clarification; Lemon juice; Fouling; Blend membranes

1. Introduction

Fruit juice is an excellent source of essential nutrients for human being. This product, obtained from the fruit by mechanical processes, has distinctiveness of color and flavor characteristic of the fruit which come from. Fruit juices contain antioxidants (vitamins, minerals, and other compounds) which are beneficial to human health. These compounds do not only reduce the risk of oxidation and damages associated with the presence of radical free, but also the risk of various types of cancer, cardiovascular, and neurological diseases. Unfortunately, the content of insoluble solids in the fruit pulp make it a very attractive environment for the growth of micro-organisms, so it requires heat treatment (115°C or more) for proper control of the microbial invasion. In general, the industrial juice loses some nutritional properties (vitamins, minerals, and enzymes) during the elaboration process to which raw materials are subjected. At present, there is a growing demand in obtaining fruit juices with original fresh features and free of chemical additives. This results in the search of new technologies that are capable of improving the nutritional and microbiological quality of the juices [1]. Conventional heat treatment, guarantees safety, and extends the shelf life of fruit juices, but often leads to damage the

*Corresponding author.

nutritional properties of the product. The technology of membrane, such as microfiltration (MF), ultrafiltration (UF), and nanofiltration may be an alternative for the preservation and conservation of fruit juices. The benefits of this technology are primarily based on the ability to operate at low temperatures and pressures, allowing savings in energy consumption, disposal of effluents, simplicity, and easy change of scale. At the same time, this technology improves the organoleptic properties of the final product [2–8]. MF is a membrane separation process driven by pressure, which allows to clarify fruit without enzymatic treatment [9], but has a great disadvantage which is the membrane fouling, resulting in the decrease of the permeate flux [1]. Membrane fouling is a factor that reduces productivity affecting the economic viability of the process.

In recent years, various articles related to the applications of UF and MF membranes in the clarification of fruit juices have been published. General discusses the influence of the pore size of the membrane and transmembrane applied pressure. Cassano et al. [10] studied the effect of transmembrane pressure, temperature, and feed flow, in the clarification of orange juice by cross-flow UF with polyvinylidenefluoride (PVDF) membranes. They obtained an orange juice clarified without the presence of insoluble solids and with physicochemical and nutritional properties comparable to natural fruit juice. The permeate flux decrease during the UF process was attributed to the membrane fouling due to the partial and total pore membrane blockage. Villant et al. [7] worked in the clarification of melon juice by cross-flow MF obtaining a juice with similar characteristics to the original juice, except for suspended solids and carotenoids. Carvalho et al. [11] evaluated the loss of sugars (glucose, fructose, and sucrose) in the clarification of pineapple juice. They used MF and UF membranes of polysulfone (PS), polyethersulfone, and PVDF in two modules of different geometries (tubular and plate/frame) to select the best process that preserves nutrients. The results demonstrated that both the membrane pore diameter and geometry module, influence the content of sugar in clarified juice. Tasselli et al. [12] assessed the performance of hollow fiber membrane in the clarification of kiwi juice. They determined the effect of transmembrane pressure, feed flow, temperature, and concentration of suspended solids on the permeate flow. In the best operational condition ($p = 75$ kPa, $T = 25$°C and $Q_f = 40$ l/h), the concentration of suspended solids in the permeate was 10% w/w. They also studied the reduction of permeate flux through the model of series resistances and ensure that at low pressures ($\Delta p < 30$ kPa) permeate flux is controlled by the intrinsic resistance of the membrane, while at higher pressures it is controlled by fouling resistance. De Bruijn et al. [13] studied the performance of different zirconium oxide UF membranes for the clarification of apple juice. They examined the effect of feed velocity, pressure transmembrane, and molecular weight cut-off on membranes fouling. Results showed that the fouling of membranes decreases at high-feed rates and low-transmembrane pressure ($V = 7$ m/s, $p = 150$ kPa). Pagliero et al. [14] in their study on orange juice clarification by cross-flow MF, showed high yields on both permeate flux and clarified juice quality when PVDF/PMMA lab made membrane where used. Chornomaz et al. [15] prepared two UF membranes from PS and PVDF in order to determine their structural characteristics and to evaluate their efficiency in lemon juice clarification. PS membrane showed higher final permeates juice flux (20.59 L/hm^2) and less fouling compared to the PVDF membrane.

As a continuation of previous research [15], the main objective of this work is to evaluate the efficiency of tangential MF/UF process to obtain clarified and stabilized lemon juice, using three different lab made membranes. It is evaluated the effect of the fluid dynamic parameters (transmembrane pressure and feed flow velocity) on the performance of permeate flux and juice quality. Finally, mathematical models to interpret the permeate flux decay with the operation time are analyzed.

2. Materials and methods

2.1. Lemon juice physicochemical parameters

Raw lemon juice was obtained by squeezing fresh lemons with a squeezer machine, then filtering it with a mesh 400 Tyler, removing complete particles with size higher than 38 μm, approximately. The sieve juice was finally storing it at −18°C. Particle size distributions of fresh juice samples were measured using a laser particle size analyzer (Mastersizer 2000, Malvern, UK). A monomodal distribution of suspended particles and high-molecular weight compounds was obtained for the sieved juice. About 85% of solid particulates were observed to possess particle sizes between 0.35 and 20.3 μm, with an average particle size around 2 μm. The feed and permeate juice was characterized by its content of soluble solids, content of total solids, titration acidity, and pH value. The soluble solids (SS) content was directly evaluated on Brix by an ARTAGO RX-5000 refractometer. The titratable acidity expressed as citric acid (%) was determined with sodium hydroxide 0.1 N by acid-base titration of lemon juice samples. For that, 5 mL of sample material

was poured in a 50 mL flask and a given volume (45 mL) of distilled water is added. A sample of 10 mL of the solution is taken and transferred to an Erlenmeyer containing 70 mL of distilled water with 0.3 mL of phenolphthalein. The sample titration was determined by NaOH 0.1 N and the citric acid percentage evaluated from

$$\%\ \text{citric acid} = \frac{V_{\text{NaOH}} \times PM_{\text{citric ac}} \times f_{\text{d}}}{n^{\text{o}}\text{eq} \times 1,000} \quad (1)$$

where f_{d} is dilution factor.

The pH value was measured with a CHECKER pocket-sized pH meter. The content of total solids (TS) was determinate by taking a sample of a given amount of lemon juice, which was weighted (m_i), and centrifuged during 15 min at 3,300 rpm. The supernatant was drained placing the test tube down for 10 min. The dry residue was weighted (m_{d}) and the percent of total solids was determined from:

$$\%\ \text{ST} = \frac{m_{\text{d}}}{m_i} \times 100 \quad (2)$$

2.2. Membrane preparation

Three different lab made asymmetric polymeric membranes were used for the lemon juice clarification tests. Flat asymmetric membranes were prepared by phase inversion technique. Casting solution consisted of different percentage of PVDF, polymethylmetacrylate (PMMA), and polyvinylpirrolidone (PVP) in dimethylformamide (DMF) solvent. The polymer solution was casted onto a non-woven Viledon polymeric flat support at 25˚C in air (45–50% relative humidity), using a film extensor with a 400 μm knife gap. Then, the nascent membrane was immersed in bi-distilled water coagulation bath and transferred to fresh distilled water during 24 h. The asymmetric membranes were dried at room temperature for 48 h before being used. Table 1 shows the different PVDF/PMMA/PVP/DMF membrane weight percentages used in the preparation of each membrane. The viscosity measurements of the cast solutions were carried out using a DVIII-Brookfield viscometer at 25˚C.

2.3. Membrane characterization

The effects of the amount of PVDF/PMMA/PVP content on the structure, hydrophilicity and functionality of the membranes were analyzed by scanning electron microscope (SEM) micrographs, air–liquid displacement, contact angle measurements, and water permeability.

2.3.1. Morphological characterization

To investigate the morphology of membranes, micrographs were obtained by a SEM LEO 1450VP. For the SEM morphological cross-section analysis, the polymeric films were fractured into liquid nitrogen, coated by sputtering a thin gold layer, and mounted on sample holder. SEM images were examined under high vacuum applying an acceleration voltage of 15 kV.

2.3.2. Pore size distribution

The pore radius distribution and mean pore radius size were determined by liquid–liquid displacement porosimetry (LLDP) technique. Three liquids (mixture of isobutanol/methanol/water; 15/7/25, v/v/v, surface tension $\gamma = 0.35$ mN/m) were used to pore analysis by applying relatively low pressures. Procedure consists on filling the membrane with a liquid (wetting liquid, aqueous phase) and then displacing it from pores with the organic phase (isobutanol saturated with water and methanol). Flux through the membrane is obtained using a syringe pump (ISCO 500D) to gradually increment the flux on the organic-phase side. Simultaneously, equilibrium pressure is measured in each incremental stage using a pressure transducer (OMEGA DP200). When the flux through the membrane reached stationary state at each applied pressure, the radii of opened pores can be calculated from Cantor's equation, assuming the liquid effectively wets the membrane (i.e. with null contact angle), as follows:

$$r_{\text{p}} = \frac{2\gamma}{\Delta p} \quad (3)$$

Table 1
Polymer and solvent composition of the synthesized membranes

Membrane	PVDF (w/w%)	PMMA (w/w%)	PVP (w/w%)	DMF (w/w%)	Viscosity (Pa s)
M1	15	5	5	75	7.15
M2	15	7	3	75	7.08
M3	18	0	5	77	7.80

where Δp is the applied pressure, and r_p is the pore equivalent pore radius. Assuming cylindrical pores, Hagen–Poiseuille relationship can be used to correlate volumetric flow (Q_i) of the pushing liquid and the number of pores, n_k ($k = 1, \ldots i$) having pore radii, r_k ($<r_i$). For each pressure step, Δp_i, the corresponding measured volume flow is correlated with the number of pores thus opened according to [16].

$$Q_i = \frac{dJ_{vi}}{d\Delta p_i} = \sum_{k=1}^{i} \frac{n_k \pi r_k^4 \Delta p_i}{8\eta l} \tag{4}$$

where l is the pore length which corresponds to the active layer thickness and η the displacing fluid viscosity. In order to obtain the distribution of pore numbers as a function of pore radius, the following expression is used:

$$\frac{dn_i}{dr_{pi}} = -\frac{\eta l \Delta p_i^6}{16\pi\gamma^6} \frac{d^2 J_{vi}}{d\Delta p_i^2} \tag{5}$$

2.3.3. Contact angle measurements

The hydrophobic character of the membranes was determined by measuring the water-membrane contact angle (θ) by the sessile-drop technique using a contact angle device (Micromeritics Instrument Corporation, Norcross, GA, USA). Three drops of water were measured for each membrane sample. The contact angle value was measured 3 min after dropping water on the membrane surface. The average contact angles (θ) were evaluated from the following expression (user manual of Micromeritics' contact angle device):

$$\cos\theta = 1 - \sqrt{\frac{Bh^2}{(1 - \frac{Bh^2}{2})}} \tag{6}$$

where $B = \rho g/2\gamma$, being "g" the gravity acceleration (980 cm/s^2), "ρ" bide stilled water density (0.9971 g/cm^3), "γ" interfacial tension of bi-distilled water (71.97 erg/cm^2), and h the height of the liquid drop.

2.3.4. Water permeability and lemon juice clarification

The filtration setup used has been described elsewhere [14] and it is shown in Fig. 1, in which the hydraulic permeability and juice filtration experiments have been performed in a cross-flow filtration cell with an effective membrane area of $A = 6.9 \times 10^{-3}$ m^2. Membrane hydraulic permeability (L_h) at $T = 20$°C was

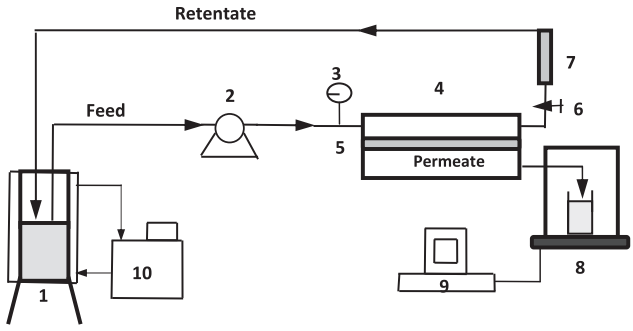

Fig. 1. Schematic diagram of the MF system: (1) feed-retentate reservoir, (2) feed pump, (3) pressure gauge, (4) permeation cell, (5) membrane, (6) needle valve, (7) flowmeter, (8) analytical balance, (9) computer, (10) thermostatic bath.

determined by measuring the permeate flow of pure water per area unit J (L/hm^2) as a function of transmembrane pressure (Δp) according to the following experimental protocol: first, the membrane was compacted at a transmembrane pressure of 1 bar for 30 min. Then, the permeate water flux J (L/hm^2) was determined by time weighing the permeate water with the analytical balance and processed with computer software, according to:

$$J = \frac{1}{A}\frac{\Delta m}{\rho \Delta t} \tag{7}$$

where Δm the permeate mass accumulated during the operation time Δt, ρ the water density (0.997 g/mL), and A the effective membrane area. The hydraulic permeability L_h (L/hm^2 bar) was calculated from the slope of J vs. Δp.

To determine the permeate lemon juice flux; the same permeation device shown in Fig. 1 was used. First membrane compaction was made with deionized water under $\Delta p = 1$ bar during 30 min. Then, the feed juice solution was pumped continuously through the MF unit from a reservoir by means of a peristaltic pump at a predetermined cross-flow velocity v and transmembrane pressure Δp. To avoid possible loss of aromatic compounds and energy saving reasons, all the experimental tests were performed at $T = 20$°C. Each test was carried out during approximately 80–90 min with total retentate recycling. The operating pressure ($\Delta p = 0.4$, 0.6, and 1 bar) and the cross-flow velocity ($v = 0.2$, 0.5, and 1.0 m/s) were maintained constant by the pump controller and the needle valve located in the outer string. During the lemon juice clarification tests, feed flow rate was measured with the flowmeter

and the collected permeate mass data were processed as volume of accumulated permeate J (L/hm^2) versus time using Eq. (7). All permeation trials were carried out in triplicate. After each juice MF experiment, the fouled membrane was rinsed with 2% (wt/wt) enzymatic detergent solution for 30 min, followed by rinsing with distilled water for 30 min and the water permeability at $T = 20$ ℃ was measured. If necessary, the cleaning procedure was repeated until the hydraulic permeability of the cleaned membrane was within 95–100% to that of the original membrane.

3. Results and discussion

3.1. Structural and physical characteristics of synthesized membranes

Fig. 2(a) and (b) shows the SEM microphotographs of M3 and M2 membrane cross sections, in which the structure change of membranes can be observed.

Similar SEM image of M2 membrane was obtained for the M1 membrane. All synthesized membranes showed asymmetric morphology consisting of a top dense layer and a highly macroporous substructure underneath. It may be noted that there is a variation of the membrane substructure from a finger-like morphology type for the M3 membrane (18% PVDF) to a less dense substructure with high macrovoids for the membrane with PMMA (15% PVDF–7% PMMA). This macrovoids structure could enhance the membrane resistance to permeation due to compaction effect. The development of macrovoids can be expected considering the decrease in viscosity values of casting solutions (Table 1), especially when the polymer solutions are prepared from different polymer concentration [17].

Structural characteristics (mean pore size, surface porosity) and contact angle are included in Table 2. The mean pore size (r_{pm}) and the porosity (ε) of the membranes were evaluated from the LLDP permeability data according to Eq. (5).

Fig. 3 shows a representative pore size distribution of M3 membrane, with a mean pore diameter in the range of MF–UF process ($r_p \approx 0.015$ μm). This distribution has been achieved by accounting for the contribution of each experimental step of flow-pressure increment to the overall membrane permeability (Eq. 5). Generally, studies indicate that the increasing the concentration of the primarily polymer in the casting solution used in the phase inversion process, leads to a reduction of pore size of the dense layer. M1 and M2 membrane mean pores radii (0.25–0.23 μm) are more than one order of magnitude higher than M3 membrane (0.015 μm). This decrease of M3 pore size can be ascribed to the higher PVDF mass in the M3 casting solution (higher viscosity). As it is commonly pointed out in literature [17], an increase in the viscosity of the casting solution causes kinetic hindrance against phase separation leading to a reduction of pore size. It can be observed that membranes pore sizes are in the suitable range for juice clarification and microbial agent retention.

The contact angle is a regular measure of the surface hydrophobicity. The values of contact angle indicate the hydrophilic character of PVDF/PMMA and PVDF membranes. M1 ($\theta = 66$) and M2 ($\theta = 64$) contact angles are lower than M3 ($\theta = 78$) one,

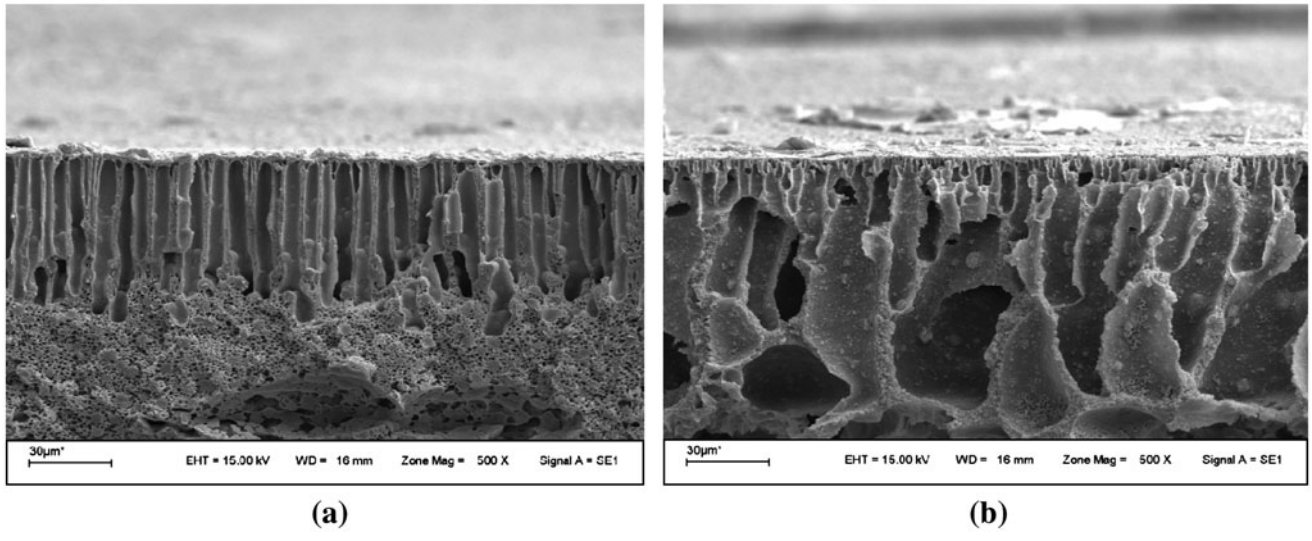

Fig. 2. SEM cross-section images: (a) M3 membrane; (b) M2 membrane.

Table 2
Membrane structural parameters, hydraulic permeability, and contact angle

Membranes	r_{pm} (μm)	ε	$L_h \pm \Delta L_h$ (L/hm^2 bar)	$\theta \pm \Delta\theta$
M1	0.251	0.25	957 ± 40	66 ± 3.0
M2	0.230	0.16	420 ± 24	64 ± 3.4
M3	0.015	0.34	252 ± 15	78 ± 4.2

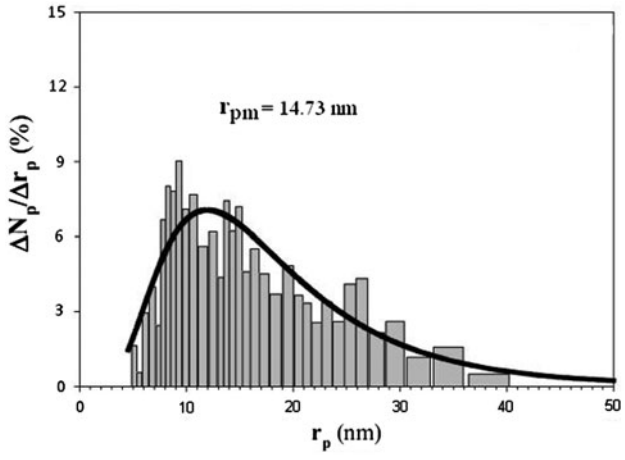

Fig. 3. Pore radius distribution from LLDP of M1 membrane.

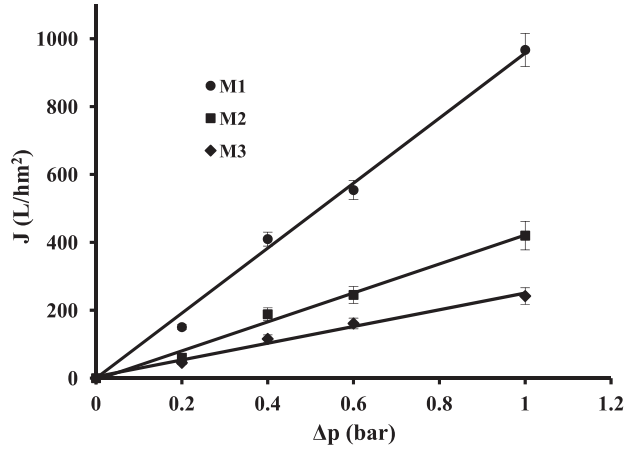

Fig. 4. Water flux of M1, M2, and M3 membranes at different transmembrane pressure.

denoting the higher hydrophilic surface character of PVDF/PMMA membranes, favoring permeation of polar water solvent. It is known that PVP performs as a pore maker when it is added in the casting solutions. Depending on the PVP content, thermodynamic or rheological factors will have a more important impact on the morphology and performance of the membrane [18]. Table 2 shows a relatively high porosity of M1 ($\varepsilon = 0.25$) and M3 ($\varepsilon = 0.34$) membranes compared with M2 ($\varepsilon = 0.16$). As expected higher membrane porosity is achieved when higher amount of PVP (5%) is used.

The average hydraulic permeabilities at 20°C obtained from the slope of permeate water flux vs. transmembrane pressure (Fig. 4) are given in Table 2. The hydraulic permeability is strongly dependent on both the hydrophilicity and the structural characteristics (pore size, porosity) of the membrane. M1 hydraulic permeability (957 L/hm^2 bar) was 2.3 and 3.8 times higher than M2 and M3 membranes, respectively. This high M1 hydraulic permeability can be in part attributed to the high-membrane surface porosity, mean pore size, and hydrophilic character.

3.2. Effect of feed velocity and pressure on permeate flux and juice quality

The permeate flux decline during the operating time is important because it lowers the filtration membrane performance. The permeate flux data as a function of operational time at feed flow rate $v = 1$ m/s and $\Delta p = 1$ bar are reported in Fig. 5.

Similar flux decline behavior from other experimental runs ($v = 0.2$–0.5 m/s and $\Delta p = 0.4$–0.6 bar) was observed. For all the runs, the permeate flux decreased considerably during the first 10–15 min and after 20 min of filtration process. The marked decrease in the permeate juice flux at the beginning of juice filtration operation, about 10–24 times lower compare with pure water flux, indicates a strong likelihood of prompt fouling and pore blocking. Prompt fouling is an adsorption phenomenon, and it is a very common effect in the MF–UF membranes. A less pronounced flux decay followed by the achievement a pseudo-steady-state (at $t \approx 40$ min) is observed. This behavior implies that the membrane resistance changes during the MF fouling. The decrease in flux with the operational time can be caused by several factors, such as concentration polarization, adsorption, pore blocking,

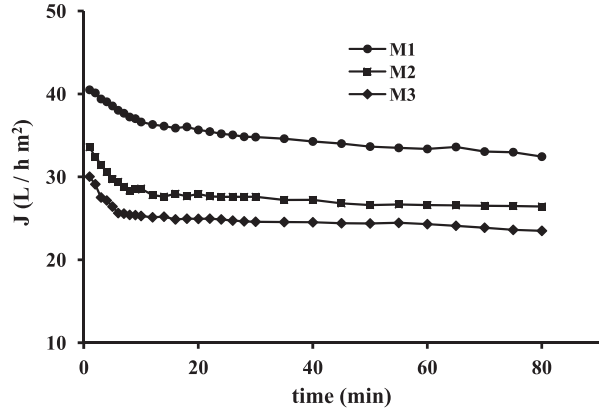

Fig. 5. Time dependence of permeate juice flux for M1, M2, and M3 membranes at $v = 1$ m/s and $\Delta p = 1$ bar.

development of a protein gel layer at the membrane surface, etc.

Fig. 6(a)–(c) shows the average pseudo-steady-state fluxes or limiting flux (J_∞) at 80 min of operation time and different operational conditions. It is clear from these figures that at pressures higher than 0.6 bar, for a given feed-flow velocity, the pressure increase determines no significant increase of the permeate flux (J_∞). This behavior could be explained by two main opposite factors: the increase of the driving force (Δp) leads to a higher permeate flux through the membrane pore and simultaneously it causes a major compaction of the deposited solutes layer on the membrane surface, leading to an augment of the fouling resistance and a decay in the permeate flux. The feed tangential velocity affects the liquid turbulence and mixing on the membrane surface. As expected, the permeate flux increased with higher operating tangential velocities, due to the increase of the shear stress at the membrane surface and, consequently, this effect enhances the rate of removal of deposited solutes responsible of flux decay. The initial and limiting permeate fluxes (at 80 min) for the best operational conditions ($v = 1$ m/s, $\Delta p = 1$ bar) of the three synthesized membranes are summarized in Table 3.

Physicochemical characteristics from feed and permeate solutions are also reported in Table 3. It can be noticed the lemon juice physicochemical characteristics of the M1, M2, and M3 are almost similar. The experimental data showed that the clarify lemon juice exhibited a total rejection of total solids and practically the same physicochemical properties (citric acid, SS, and pH) than those of the original lemon juice. These results indicate that the M1 membrane presents the best performance, higher both permeate flux (32.5 L/hm^2) and juice quality.

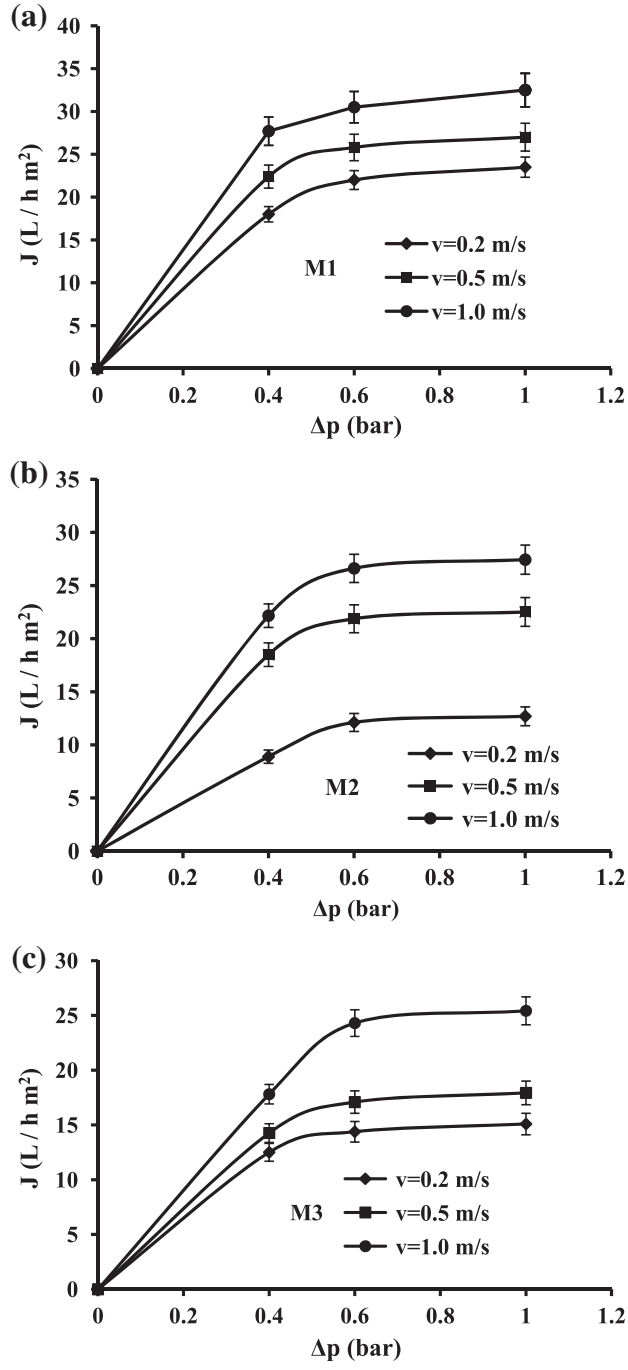

Fig. 6. Effect of feed flow velocity and transmembrane pressure on limiting permeate fluxes (at 80 min) of: (a) M1; (b) M2; (c) M3 membranes.

After each cleaning procedure, the hydraulic permeabilities at $T = 20$°C of the treated membranes were evaluated. The L_h values of the cleaned membranes were somewhat lower (≈5%) than those of the original membrane. This suggests that after the

Table 3
Flux and physicochemical values of juice solutions ($\Delta p = 1$ bar; $v = 1$ m/s)

Membranes		M1	M2	M3
Permeate flux	J_0 [L/hm^2]	40.50	33.58	30.03
	J_∞ [L/hm^2]	32.50	26.40	23.50
%citric acid	Feed	7.76	7.62	7.40
	Permeate	7.55	7.50	7.27
%ST	Feed	0.97	1.02	0.95
	Permeate	0	0	0
%SS	Feed	8.04	7.82	7.97
	Permeate	7.73	7.45	7.85
pH	Feed	2.04	2.16	2.23
	Permeate	2.03	2.34	2.36

cleaning procedure the surface and/or the porous structure of the original membrane were practically unmodified.

3.3. Membrane fouling interpretation

According to the early works on flux decline dynamics, fouling of porous membranes can be attributed to several more or less independent but generally coexisting phenomena, involving solute adsorption onto the membrane surface, pore blocking, concentration polarization, and cake layer formation. The sharp decrease of permeate juice flux during the first 10 min is usually attributed to pore blocking and the growth deposition of a gel layer formed by cellulose, hemicelluloses, and high-molecular weight compounds (polysaccharides, protein, colloidal materials, etc.) present in the juice. Considering the mean pore size of these membranes (0.25–0.015 μm) and the relative large size of the solutes (average particle size ≈2 μm), it can be assumed that each particle or solid compound that reaches the membrane surface plug completely the pore, diminishing the pore surface area. The pore blocking takes place on the membrane surface and not inside the pores (the solute is larger than pore size). This fouling mechanism is so-called complete blocking and the equation that governs this model is [19]:

$$\ln J = \ln J_0 - k_1 t \tag{8}$$

where the k_1 parameter is related to the number of pores per surface unit blocked per unit of filtered volume. After a few minutes of filtration process, these solutes deposition on the surface form a secondary dynamic membrane as the MF goes on, increasing the total membrane resistance, probably being this mechanisms the mainly resistance controlling the permeate flux. In this case, the flux time dependence is given by the following expression:

$$\frac{1}{J^2} = \frac{1}{J_0^2} + k_2 t \tag{9}$$

where J_0 is the initial flux and k_2 a phenomenological characteristic coefficient, parameter which is related to the apparent specific resistance of the cake and to the cake mass per unit of permeated volume.

From this assumption, the criterion it has been used in the theoretical interpretation of the flux decline was to fit with Eqs. (8) and (9) with experimental data included within the interval of time in which the correlation coefficients were $R^2 \geq 0.90$. Figs. 7

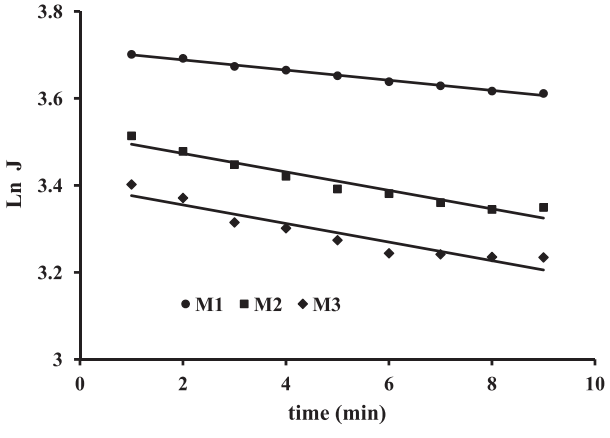

Fig. 7. Complete blocking model fitting (straight lines) to the experimental data (symbols) at $v = 1$ m/s and $\Delta p = 1$ bar.

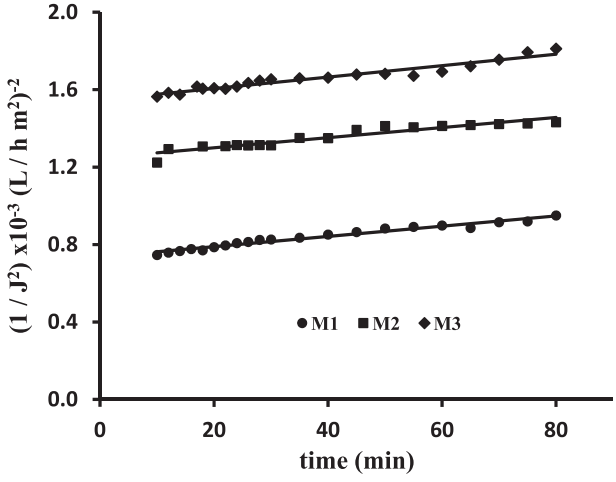

Fig. 8. Cake model fitting (straight lines) to the experimental data (symbols) at $v = 1$ m/s and $\Delta p = 1$ bar.

Table 4
k and J_0 parameters of fouling models ($v = 1$ m/s, $\Delta p = 1$ bar)

		Complete blocking (Eq. 8)			Cake (Eq. 9)		
Membrane	J_0 (exp) [L/hm^2]	J_0 [L/hm^2]	$k_1 \times 10^2$	R^2	J_0 [L/hm^2]	$k_2 \times 10^5$	R^2
M1	40.50	40.85	1.17	0.99	37.34	0.265	0.97
M2	33.58	33.78	2.12	0.95	28.28	0.260	0.90
M3	30.03	29.96	2.14	0.90	25.82	0.295	0.94

and 8 show the adequate fitness of the experimental data, in the time intervals of 0–10 min and 10–80 min, for the complete blocking and cake model, respectively. In Table 4, the corresponding parameters values of k_1 and k_2 constants and initial permeate fluxes (J_0) by fitting experimental data with the models according to Eqs. (8) and (9) are tabulated. The value of complete blocking constant is correlated with the corresponding time constant k_1 (Eq. 8). The so-obtained k_1 values show that the suspended juice solids block less surface pores of M1 membrane per unit of filtered volume compare to M2 and M3 membranes. Related to the extrapolated initial flux from the complete blocking model, they were very close to the experimental data (within 99%). The apparent specific resistance (k_2) is due to the formation of the cake, which seems to be present after 10 min of operational filtration time. The cake is raised from aggregates formed by several molecules and particles strongly linked together. The k_2 values of the three synthesized membranes do not show a substantial difference between them. This could probably be attributed to the similar properties of compact layer cakes formed or similar apparent specific resistance of the cake under the same operational conditions (pH, temperature, feed flow, and transmembrane pressure). Referring to the extrapolated initial permeate fluxes, they were 8–15% lower than those of the experimental initial permeate fluxes. This can be ascribed to that when the cake fouling begins to overcome the initial flux has diminished due to the preceding blocking fouling. These results suggest that during the first 10 min of operational time the complete blocking is the predominant fouling mechanism and after that the cake fouling appears as the dominant mass transfer mechanism through the membrane.

4. Conclusions

The performance in clarifying lemon juice of three different MF polymeric membranes made in our laboratory was investigated. The MF membranes were prepared by the inversion phase technique from casting solutions containing different amounts of PVDF, PMMA, and PVP polymers. The best performance–both permeate flux and juice quality—was obtained with blend membrane containing 15% of PVDF, 5% PMMA, and 5% PVP, achieving a limiting permeate flux of 32.5 L/hm^2 at $\Delta p = 1$ bar and $v = 1$ m/s, whereas the total solids were completely removed. Experimental decay of permeate fluxes was interpreted in terms of the blocking and cake fouling mechanisms. Good correlations between the experimental data and theoretical fitting were achieved. It has been shown that the fouling phenomenon mainly occurs externally onto the membrane surface. The results suggest that after 10 min of operating time the cake fouling appears as dominant mechanisms of mass transfer through the membranes.

Acknowledgments

The authors acknowledge the National Research Council of Argentina (CONICET) and National Agency for Scientific Promotion (ANPCyT) for their financial support.

References

[1] L. Carneiro, I. dos Santos Sa, F. dos Santos Gomes, V.M. Matta, Cold sterilization and clarification of pineapple juice by tangential microfiltration, Desalination 148 (2002) 93–98.
[2] S.S. Koseoglu, J.L. Lawhon, E.W. Lusas, Use of membranes in citrus juice processing, Food Technol. 44 (1990) 90–97.
[3] G. Capannelli, A. Bottino, S. Munari, D.G. Lister, G. Maschio, I. Becchi, The use of membrane processes in the clarification of orange and lemon juices, J. Food Eng. 21 (1994) 473–483.
[4] S. Todisco, L. Peña, E. Drioli, P. Tallarico, Analysis of the fouling mechanism in microfiltration of orange juice, J. Food Process. Preserv. 20 (1996) 453–466.
[5] A. Laorko, Z. Li, S. Tongchitpakdee, S. Chantachum, W. Youravong, Effect of membrane property and operating conditions on phytochemical properties and

permeate flux during clarification of pineapple juice, J. Food Eng. 100 (2010) 514–521.
[6] A. Cassano, E. Drioli, G. Galaverna, R. Marchelli, G. Di Silvestro, P. Cagnasso, Clarification and concentration of citrus and carrot juices by integrated membrane processes, J. Food Eng. 57 (2003) 153–163.
[7] F. Vaillant, M. Cisse, M. Chaverri, A. Perez, M. Dornier, F. Viquez, C. Dhuique-Mayer, Clarification and concentration of melon juice using membrane processes, Innovative Food Sci. Emerg. Technol. 6 (2005) 213–220.
[8] D.S. Couto, M. Dornier, D. Pallet, M. Reynes, D. Dijoux, S.P. Freitas, L.M.C. Cabral, Evaluation of nanofi ltration membranes for the retention of anthocyanins of açai (*Euterpe oleracea Mart*.) juice, Desalin. Water Treat. 27 (2011) 108–113.
[9] H. Mirsaeedghazi, Z. Emam-Djomeh, S.M. Mousavi, A. Aroujalian, M. Navidbakhsh, Clarification of pomegranate juice by microfiltration with PVDF membranes, Desalination 264 (2010) 243–248.
[10] A. Cassano, M. Marchio, E. Drioli, Clarification of blood orange juice by ultrafiltration: Analyses of operating parameters, membrane fouling and juice quality, Desalination 212 (2007) 15–27.
[11] L.M.J. de Carvalho, I. de Castro, C.A. Da Silva, A study of retention of sugars in the process of clarification of pineapple juice (*Ananas comosus*, *L. Merril*) by micro- and ultra-filtration, J. Food Eng. 87 (2008) 447–454.
[12] F. Tasselli, A. Cassano, E. Drioli, Ultrafiltration of kiwifruit juice using modified poly(ether ether ketone) hollow fibre membranes, Sep. Purif. Technol. 57 (2007) 94–102.
[13] J. De Bruijn, A. Venegas, R. Borquez, Influence of crossflow ultrafiltration on membrane fouling and apple juice quality, Desalination 148 (2002) 13l–l36.
[14] C. Pagliero, N.A. Ochoa, J. Marchese, Orange juice clarification by microfiltration: Effect of operational variables on membrane fouling, Latin Am. Appl. Res. 41 (2011) 279–284.
[15] P.M. Chornomaz, N.A. Ochoa, C. Pagliero, J. Marchese, Synthesis, characterization and performance of membranes for clarification of lemon juice, Desalin. Water Treat. 28 (2011) 1–5.
[16] L.R. Firman, N.A. Ochoa, J. Marchese, C.L. Pagliero, Deacidification and solvent recovery of soybean oil by nanofiltration membranes, J. Membr. Sci. 431 (2013) 187–196.
[17] N.A. Ochoa, M. Masuelli, J. Marchese, Effect of hydrophilicity on fouling of an emulsified oil wastewater with PVDF/PMMA membranes, J. Membr. Sci. 226 (2003) 203–211.
[18] D. Wang, K. Li, W.K. Teo, Preparation and characterization of polyvinylidene fluoride (PVDF) hollow fiber membranes, J. Membr. Sci. 163 (1999) 211–220.
[19] C. Almandoz, C. Pagliero, A. Ochoa, J. Marchese, Corn syrup clarification by microfiltration with ceramic membranes, J. Membr. Sci. 363 (2010) 87–95.